Phys Chem Minerals (1990) 17:313–319

PHYSICS AND CHEMISTRY OF MINERALS

The System Fe – FeO Revisited

A.E. Ringwood and W. Hibberson

Research School of Earth Sciences, Australian National University, Canberra, A.C.T. 2601, Australia

Received December 12, 1989

Abstract. The results of a reconnaissance investigation of melting relationships in the system Fe – FeO at 16 GPa were recently described by Kato and Ringwood (1989). The principal sources of uncertainties in those experiments were caused by loss of FeO to sample capsules during runs and the estimation of sample temperatures by an indirect method, based upon a prior calibration of the relationship between power input and temperature. A further set of 24 runs at 16 GPa has been carried out using improved experimental techniques. The melting temperatures of iron and wüstite at 16 GPa are found to be 1945 ± 20° C and 1875 ± 25° C respectively. (Quoted errors do not include possible effects of pressure on thermocouple emf). The Fe – FeO eutectic is now located at 10 ± 2 wt% FeO and 1670 ± 20° C (previously 15.5 ± 3 wt% FeO and 1700 ± 25° C). The new determination of the depression of the melting point of iron by solution of FeO is 27.5° C/wt% FeO as compared to the previous value of 23° C/wt% FeO. The present results show that the contraction of the liquid immiscibility field in the system at high pressure is somewhat larger than was estimated previously. This study confirms the general topology of high pressure phase relationships in the Fe – FeO system obtained by Kato and Ringwood (1989) and has similar implications for the process of core formation within the Earth.

Introduction

An investigation of phase relationships in the system Fe – FeO at 16 GPa and 1600–2200° C was recently described by Kato and Ringwood (1989). This work established the essential topology of the phase diagram under these conditions. However, owing to experimental difficulties which were encountered, the work was regarded essentially as a reconnaissance study. One problem encountered during experiments on this system is the rapid exsolution of Fe and FeO which can occur during quenching, thereby complicating the interpretation of equilibrium phase relationships which had been established under the P and T conditions of the run. To facilitate these interpretations, it was found expedient to carry out runs simultaneously on two charges possessing different compositions. However, this prevented the insertion of a thermocouple during the run. Accordingly, run-temperatures were estimated from the power input, using a previous calibration of power input versus temperature as measured by a $W_{97}Re_3$-$W_{75}Re_{25}$ thermocouple. This procedure necessarily introduced larger uncertainties in run temperatures than would have otherwise occurred if thermocouples had been used in each run. A second experimental problem was caused by the high reactivity of molten FeO, some of which entered the walls of the MgO container-tubes forming magnesiowüstite solid solutions, thereby causing the bulk composition of the charge to become more iron-rich and oxygen-depleted during the course of the run. We now report the results of a further series of runs using improved experimental methods which have avoided these two particular problems.

Experimental Methods

The high P, T experiments were carried out in an MA-8 apparatus. Except for the modifications described below, the experimental procedures were identical to those described by Kato and Ringwood (1989). All runs were carried out using only a single charge, and a $W_{97}Re_3$-$W_{75}Re_{25}$ thermocouple was placed immediately adjacent to the charge. Previous experience with this assembly (Irifune and Hibberson 1985) has demonstrated that the temperature throughout the central region (dimensions 2–3 mm) of the charge is uniform and is normally determined within ±20° C. However, this does not include errors caused by the effect of pressure on thermocouple EMF. Outside this central region, a substantial temperature gradient is present. In most of the present experiments the charges were contained in thin tubes of high purity alumina. In compositions more iron-rich than $Fe_{50}FeO_{50}$ (wt%), these tubes did not react significantly with the charges during the course of the runs. At low pressures, FeO normally reacts with Al_2O_3

to form hercynite, $FeAl_2O_4$. However, most of the present experiments were carried out at a pressure (16 GPa) which was sufficiently high to cause $FeAl_2O_4$ to disproportionate into a mixture of FeO plus Al_2O_3. In some compositions rich in FeO and at temperatures above 1800° C, there was significant degree of reaction of FeO with alumina, and large anhedral crystals of corundum formed in the FeO near the capsule wall. Accordingly, results in Al_2O_3 capsules from compositions richer than 50% FeO have not been utilized in the present study. Four runs were carried out in MgO capsules in order to determine the melting point of wüstite. This was accomplished satisfactorily, despite substantial reaction of FeO with the capsule walls. A few runs were also carried out in Ca-stabilized zirconia tubes. This material can be used to contain iron-rich compositions, but seems to react with FeO-rich compositions at very high temperatures. Fortunately, FeO-rich liquids exsolved from most runs possessing bulk compositions with more than 50% metallic iron did not display significant reaction with either alumina or zirconia containers at temperatures below 1850° C. These quenched liquids typically contained less than 0.7% Al_2O_3 or ZrO_2.

After completion of the runs, the charges were quenched by turning off the power, removed from the apparatus, and studied by optical and electronprobe techniques. The melting point of pure iron (Johnson and Matthey "Specpure" grade) was also measured at 16 GPa using both Al_2O_3 and ZrO_2 capsules. Temperature was raised above 1800° C at a rate between 50 and 100° C/min and melting was detected via the observation of large discontinuous changes in electrical resistivity.

Results

The results of the present series of runs are summarized in Table 1 and a phase diagram based on these results is shown in Fig. 1. The occurrence of melting is easily recognized by a major change of texture, as compared to the subsolidus texture (Figs. 2a, 3). The nature of this change depends upon the composition of the charge in relation to the Fe–FeO eutectic. This is fortunate since it permits the position of the eutectic to be defined. In runs which are more Fe-rich than the eutectic composition, part of the dissolved FeO migrates to the margins and is precipitated as relatively large anhedral crystals during quenching, whilst the other part is precipitated more or less in place as dispersed, mostly sub-micron crystallites in a matrix of metallic iron. The result is that runs on the Fe-rich side of the eutectic contain a central, relatively clear region of metallic iron, free of large (i.e. >5 μm) primary crystals of FeO, as is seen in Fig. 3. However, in compositions which are more FeO-rich than the eutectic, the "excess" FeO (i.e., beyond the eutectic composition) crystallizes in situ as dispersed, anhedral 10–30 micron-sized crystals (Figs. 2b, 4). In a series of runs near the solidus at 1700° C, essentially complete solution of FeO in the metallic Fe-rich melt was observed for $Fe_{95}FeO_5$ and $Fe_{92.5}FeO_{7.5}$ compositions and the composition $Fe_{90}FeO_{10}$ was mainly liquid, but with a few large primary crystals FeO remaining in localized regions of the metal. In the $Fe_{87.5}FeO_{12.5}$ composition, the hottest region of the molten zone was free of FeO crystals, whilst an immediately adjoining molten region which was probably only ~20° C cooler contained dispersed, primary FeO crystals. The melted, but non-segregated region is

Table 1. Results of melting experiments in Fe–FeO system at 16 GPa using Al_2O_3 containers

Run number	Temp °C	Time seconds	Comp wt% FeO	Results
506	1600	120	10	Intimate mixture of Fe_c and FeO_c; all subsolidus.
507	1650	120	10	As for 506.
527	1675	120	10	Small molten zone in hottest region of charge.
504	1700	60	5	Extensive melting with clear central region of L_m free of primary FeO crystals and some segregation of FeO_c along margins.
505	1700	60	7.5	Similar to 504. See Figure 3.
502	1700	60	10	Extensive melting with clear regions of L_m free of primary crystals of FeO. In other regions, some primary FeO crystals were present within L_m.
512	1700	60	12.5	Extensive melting with primary FeO_c distributed throughout L_m, except in a thin strip along the hottest margin.
503	1700	60	15	Extensive melting with primary FeO_c distributed throughout L_m. See Fig. 4.
496	1700	45	47	Central region of charge melted. Primary FeO_c remained distributed throughout L_m.
498	1750	30	47	Extensive melting with densely packed primary crystals of FeO_c distributed throughout L_m.
495	1750	30	47	As for 498.
526	1775	30	47	Large ovoid blob of L_m containing innumerable exsolution droplets of quenched FeO in its interior. The blob is surrounded by a continuous quenched rim of L_o, now consisting of FeO_c with lesser amounts of dispersed Fe_c particles. This run was carried out in the liquid immiscibility field (L_m+L_o). See Figs. 2a, c, d.
493	1800	30	47	As for 526.
494	1800	30	47	As for 526.
482	1850	30	47	Similar to 526; however, quenched FeO droplets in metallic L_m blob were less abundant.
488	1900	20	47	Similar to 482, except that quenched FeO droplets in metallic L_m blob were less abundant.
492	2000	30	47	Large, irregular, partly coalesced blobs of L_m surrounded by former L_o now consisting of quenched (FeO_c+Fe_c). Quenched droplets of FeO within L_m were much less abundant than in runs 526-488. This run was probably carried out in the (L_m+L_o) liquid immiscibility field but the possibility that the texture was caused by exsolution from a homogeneous liquid during quenching cannot be excluded.

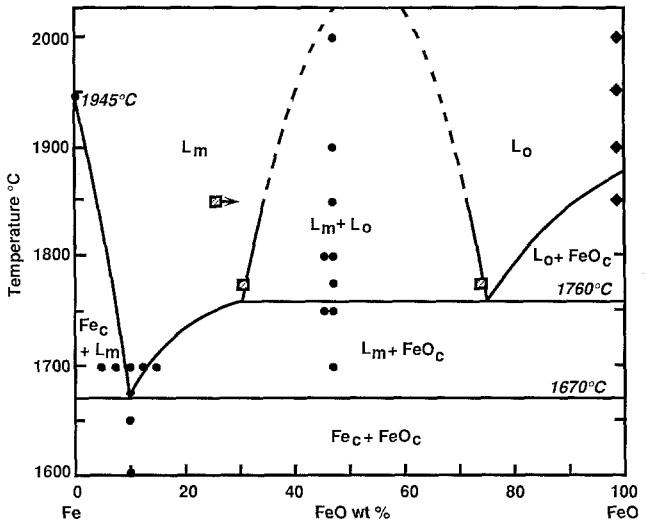

Fig. 1. Phase diagram of the system Fe–FeO at 16 GPa based upon the present experiments. *Solid circles* denote the compositions and temperatures of individual runs in alumina capsules. *Solid diamonds* denote runs in MgO capsules. *Squares* denote the compositions of equilibrium liquids determined by point-counting of photographs of quenched charges

interpreted as lying marginally on the FeO side of the eutectic (see Fig. 1) whilst at a slightly higher temperature, complete melting had occurred, yielding a region of clear metal. In $Fe_{85}FeO_{15}$ and $Fe_{53}FeO_{47}$ compositions, large amounts of FeO crystals remained distributed throughout the metallic iron (Figs. 2b, 4). These observations indicate that the eutectic composition contains more than 7.5% FeO, less than 15% FeO, and probably slightly less than 12.5% FeO. Our preferred estimate of the eutectic composition (at 16 GPa) is $10\pm$ 2% FeO. This estimate is supported by electronprobe analyses of the oxygen content of the metal phase, described subsequently. The solidus (eutectic) temperature is located on the basis of these textural observations to lie just below 1675° C and above 1650° C at 16 GPa and between 1550–1600° C at 10 GPa. We estimate the solidus to lie at 1670 ± 20° C at 16 GPa.

In the following discussion, the symbol L_m is used to denote the metallic liquid comprised of molten iron which has dissolved varying amounts of FeO, whilst L_o denotes the oxide liquid comprised mainly of molten FeO which has dissolved varying amounts of excess iron. Crystalline wüstite is denoted as FeO_c. (See Ringwood (1984) and Kato and Ringwood (1989) for explanations of this terminology). The field of ($L_m + FeO_c$) extends from the solidus to just above 1750° C, as shown in Fig. 1. At 1775° C, melting of FeO occurs and a field of liquid immiscibility ($L_m + L_o$) is entered (Fig. 2). There is a drastic change in the textures of quenched runs at this point. The FeO-rich liquid segregates very rapidly to the margins of the charge, leaving a central metal-rich blob corresponding to the former metallic liquid, L_m. In one experiment where the cell was still being heated to the run temperature, a blowout occurred causing almost instantaneous quenching of the charge. Nevertheless, complete segregation of the two liquids had already occurred, demonstrating that this process occurs very rapidly once the liquid immiscibility field is entered. In contrast, below this region, in the ($FeO_c + L_m$) field, segregation of crystalline FeO from L_m does not occur.

At temperatures between 1775–1850° C, FeO formerly dissolved in the central regions of the liquid metal blob exsolves during quenching to form a cloud of FeO droplets, mostly in the size-range 5–15 μm (Fig. 2a, c). The composition of the equilibrium metallic liquid (L_m) at 1775° C was determined by point-counting of the quenched products to have contained 31% FeO (Fig. 2a, c). This demonstrates a rapid increase of solubility of L_o in L_m with increasing temperature (Fig. 1). In the outer zones of the metal blobs, FeO does not exsolve as droplets, but instead migrates rapidly to the margins during quenching. The textures of runs at 1800 and 1850° C generally resemble those of the 1775° C run. However, above 1850° C, lateral migration predominates during quenching, and it is no longer possible to estimate the FeO content of the equilibrium metallic liquid by point-counting. At 1850 °C, the equilibrium metallic liquid was estimated to have contained 26 wt% FeO. This is believed to represent a lower limit to the solubility of FeO under these conditions, owing to lateral migration of FeO during quenching, as described above.

Within the liquid-immiscibility field, the FeO-rich liquid (L_o) forms a rim surrounding the L_m droplet (Fig. 2a, region C). This rim quenches to an intergrowth consisting mainly of wüstite containing crystals of metallic iron (Fig. 2d). Electronprobe microanalysis indicates the composition of the wüstite is near-stoichiometric. This is supported by the results of Kato et al. (1989) which indicated a composition near $Fe_{0.97}O$. The FeO-rich immiscible liquid (L_o) at 1775° C was determined by point-counting to have contained 26 wt% of metallic iron (Fig. 2a, d). This composition lies very close to that of the ($L_o - FeO_c$) eutectic (Fig. 1).

The melting point of high-purity metallic iron (Johnson and Matthey, Specpure grade) was determined separately in Al_2O_3 and ZrO_2 containers at 16 GPa. The onset of melting was indicated by a sharp increase in resistance (Fig. 5). Essentially identical melting temperatures of 1945 ± 5° C (Al_2O_3) and 1950 ± 10° C (ZrO_2) were recorded.

Melting Point of Wüstite

It was not possible to determine the melting point of wüstite by the above methods because of reaction of FeO with the Al_2O_3 container. Instead, four runs at 1850, 1900, 1950 and 2000° C were carried out on a wüstite composition contained in MgO capsules. Run times were 30 s. The wüstite was introduced as a compositionally equivalent mixture of $Fe + Fe_2O_3$. These components react promptly ($\sim$1 min) at 900–1000° C to form wüstite during the slow heating cycle (which usually took $\sim$60 min to reach the run temperature). During this period, substantial diffusion of MgO from the capsule walls into the FeO charge took place, so that the compositions on which the melting experiments occurred were

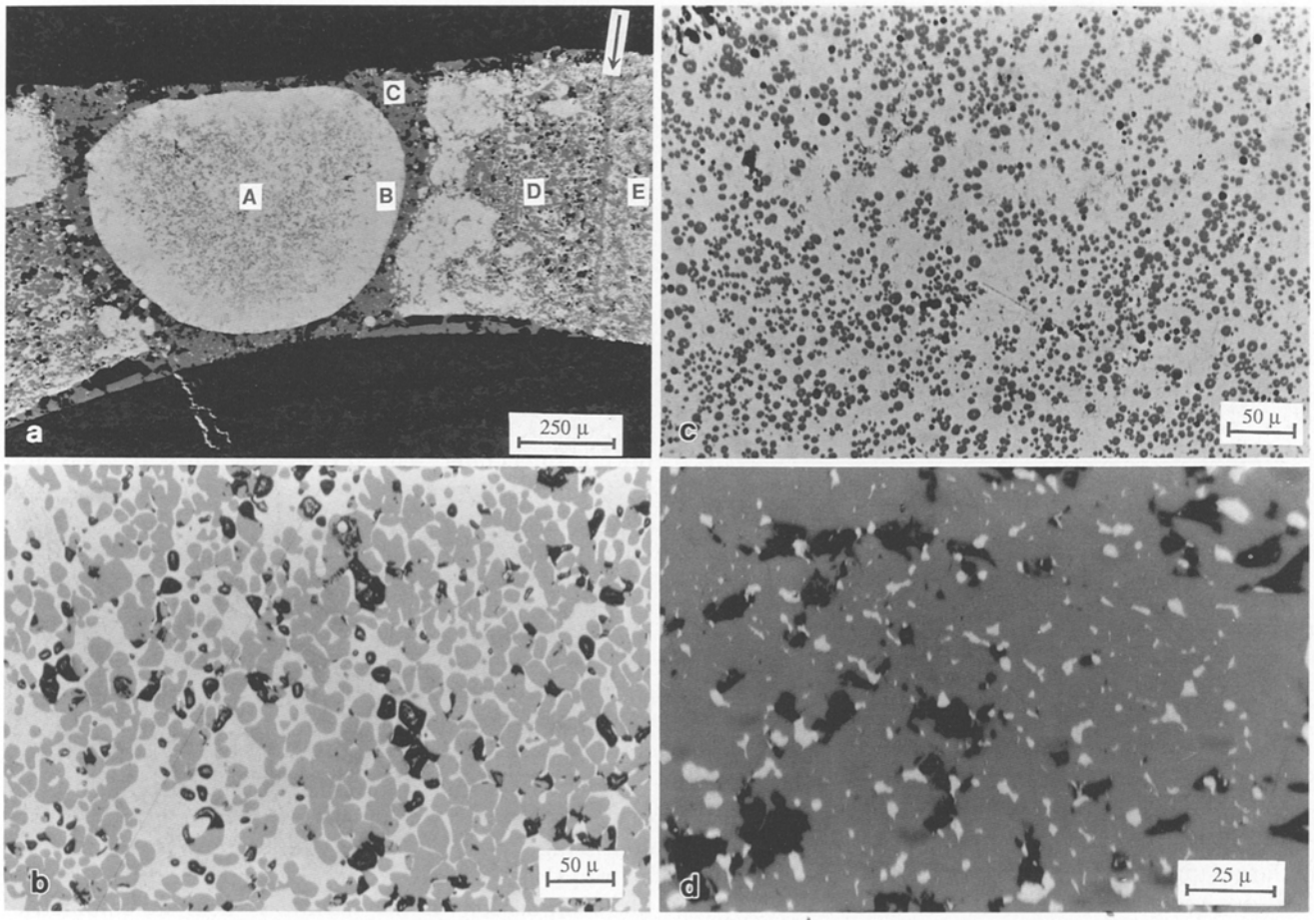

Fig. 2a. Polished section of run 526 containing 47 wt% FeO showing the effects of liquid immiscibility between a metallic iron-rich melt and an ionic FeO-rich melt. The temperature of the central region was 1775° C, and falls by about 100° C laterally away from the central blob, towards the margins of the picture. The bright central region of the charge (*A*), comprising quenched Fe-rich melt (L_m), now consists of iron peppered with innumerable (~10 μ) droplets of FeO that exsolved during quenching. Its peripheral region (*B*) is relatively free of FeO owing to outward diffusion of oxygen during quenching. The central metallic blob is surrounded by a dark shell (*C*) now comprised of a mixture mainly of FeO containing dispersed crystals of metallic iron, which corresponds to the immiscible ionic FeO-rich liquid (L_o) that was in equilibrium with the metallic melt (L_m) during the run. Further out, the region (*D*), which was at a temperature of ~1700° C can be seen to have been comprised of crystalline (primary) FeO plus Fe-rich metallic liquid. This region thus lies in the (L_m+FeO_c) field to the right of the Fe–FeO eutectic in Fig. 1. The onset of melting corresponding to the Fe–FeO eutectic temperature (1670° C) is marked by the dark, narrow, near-vertical bands rich in FeO (*arrowed*), plus a textural discontinuity between regions (*D*) and (*E*). The latter region represents the subsolidus assemblage (Fe_c+FeO_c). **b** Detail of region *D* of Fig. 2a, showing abundant primary crystals of FeO distributed throughout quenched metallic liquid (L_m). This region experienced a temperature of about 1700° C during the run and corresponds to the (FeO_c+L_m) field of Fig. 1. Note that primary FeO crystals remain in situ and do not segregate or migrate from the iron-rich liquid in this region. Note also the wetting of FeO grain boundaries by the metallic liquid phase. **c** Interior of region *A* in **a**. Numerous FeO droplets, originally dissolved in the metallic liquid have exsolved during quenching. Point-counting shows that the equilibrium metallic liquid originally contained 26 wt% of dissolved FeO. **d** Close-up of former ionic FeO-rich immiscible liquid (L_o) from region (*C*) in **a**. The liquid has quenched to an assemblage of grey wüstite and bright metallic iron. *Dark areas* are holes which developed during polishing. The bulk composition of the immiscible ionic liquid was determined by point-counting to have comprised 26 wt% Fe and 74 wt% FeO.

actually magnesiowüstite solid solutions. Most of this diffusion occurred at temperatures which were within about 50 degrees of the solidus. The diffusion was essentially undirectional. MgO diffused into the charge, but FeO did not diffuse substantially into the capsule wall. Sharp boundaries existed between the pure MgO of the capsule and the charges possessing Mg-numbers (Mg* = 100 MgO/(MgO+FeO) which ranged between 7–53. In run 555 at 1850° C the central region of the charge was homogeneous (Mg* = 7) and there was no evidence of melting. However, runs 547 and 548 at 1900° C clearly displayed partial melting. In the hottest central regions of both runs, discrete crystals of magnesiowüstite ~5 μm in diameter and with Mg*21–26 were surrounded by rims possessing Mg*4-7 which were interpreted as quenched partial melts. There was little difference between the phase compositions in both runs. However, the partially melted region was more extensive in the 1950° C run. Outside the partially melted regions, zoning of the charges caused by subsolidus inward diffu-

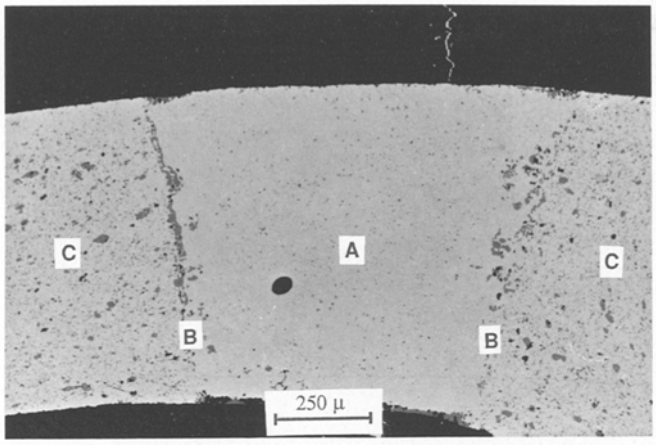

Fig. 3. Polished section of run 505 containing 7.5 wt% FeO. Central region of charge was at 1700° C. Relatively clear central region (*A*) consists of former metallic liquid (L_m) from which very fine crystallites of FeO (mainly <1 μ) have precipitated during quenching. Some FeO has also migrated laterally and precipitated along the linear boundary (*B*) marking the solidus at the eutectic temperature at 1670° C. Note the absence of large primary crystals of FeO_c, (in contrast to Figs. 2b and 4), indicating that the run crystallized in the ($Fe_c + L_m$) field on the left-hand side of the eutectic. Region *C* represents subsolidus ($Fe_c + FeO_c$)

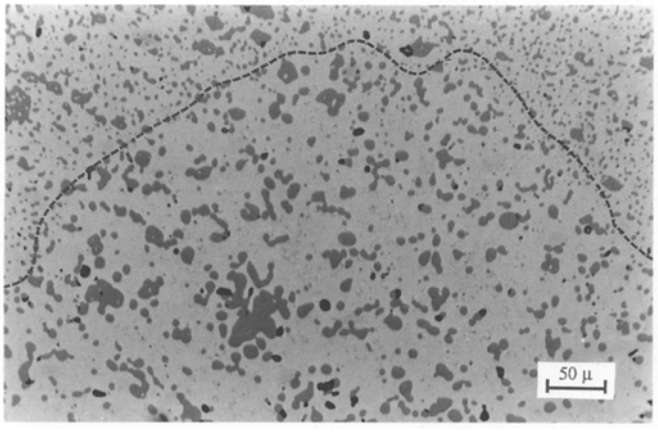

Fig. 4. Polished section of run 503 containing 15% FeO. Temperature of central melted region (outlined by *dashed curve*) was 1700° C. Recrystallized, anhedral, primary crystals of FeO_c are scattered through this region, immersed in former L_m. Note contrast with run 505 (Fig. 3) in which primary FeO crystals are absent within melted region. This run is interpreted to have crystallized in the field of ($FeO_c + L_m$) just on the right hand side of the eutectic

sion of MgO was parallel to the boundaries of the charges, with Mg* mainly between 25–40.

As charge 546 was being heated to the run temperature of 2000° C, a substantial deflection of the power versus temperature curve occurred near 1970° C, indicating abnormal endothermic behaviour and suggesting the occurrence of extensive melting. This was confirmed by examination of the charge which consisted of separate large ~20 μ crystals of magnesiowüstite (Mg* = 55) surrounded by ~5 μ rims possessing Mg*8-10. The latter clearly represent quenched, iron-rich partial melt.

Melting relationships in the iron-rich portion of the

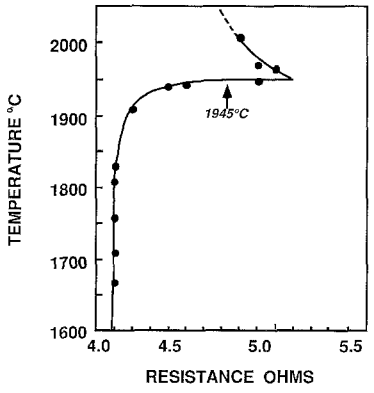

Fig. 5. Melting of pure iron at 16 GPa in an Al_2O_3 container is detected by a sharp change in electrical resistance across the charge

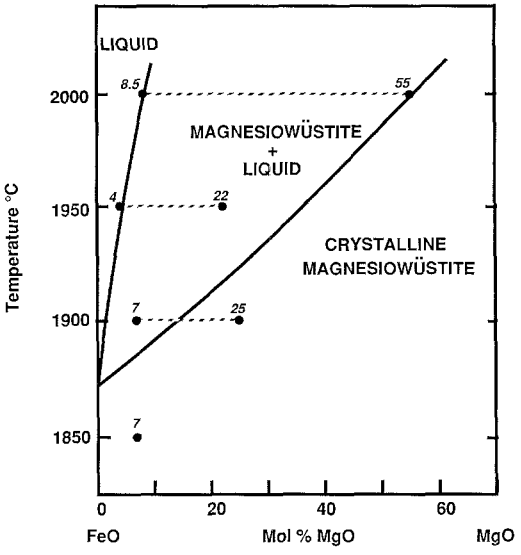

Fig. 6. Melting relationships of iron-rich magnesiowüstite solid solutions at 16 GPa and 1800–2000° C. Numbers denote compositions of Mg-rich crystals and coexisting Fe-rich quenched melt overgrowths (joined by dashed lines in above-solidus runs) as measured by electronprobe microanalyses

magnesiowüstite system at 16 GPa are illustrated in Fig. 6. The melting point of wüstite clearly lies below 1900° C whilst the solidus of magnesiowüstite (Mg* = 7) is above 1850° C. The topology of the system (Fig. 6) implies that the melting point of pure wüstite wound be close to that of the magnesiowüstite (Mg* = 7) produced in run 555. It seems likely, therefore, that the melting point of pure wüstite lies between 1850 and 1900° C at 16 GPa, but we cannot exclude the possibility that it is slightly below 1850° C (Fig. 6).

Determination of $Fe-FeO_c$ Eutectic Composition by Electronprobe Microanalysis

Electron microprobe analyses of the metallic phases in these experiments showed that they contained significant amounts of oxygen, ranging mostly between 0.5–2.2 wt% O. In bulk compositions containing more than

10% FeO, no systematic relationships were observed between oxygen content of metal and other variables such as bulk composition and run conditions. In runs containing primary FeO_c, the crystals provide nuclei around which most of the oxygen which was originally dissolved in the metal becomes precipitated (as FeO_c) during quenching, leaving variable amounts of residual O in the metal. However, in compositions containing 10% and less of FeO, some useful results were obtained, particularly at temperatures close to the solidus.

During quenching of these compositions, oxygen migrates to the margins and is precipitated as anhedral crystals of wüstite. In some runs carried out using MgO capsules, this process also occurs during the course of the run as FeO reacts with the capsule wall to form magnesiowüstite (Kato and Ringwood 1989). As oxygen migrates outwards, the central melt becomes oversaturated with metal as required by the phase relationships in Fig. 1, and crystals of iron separate, which intergrow to form a framework. Ultimately, pockets of residual liquid near the Fe–FeO eutectic composition become isolated within the framework of metallic iron crystals and diffusion of oxygen to the boundary of the charge is henceforth prevented. The trapped pockets of melt crystallize as very fine intergrowths of FeO_c and metallic iron (Fig. 7). At temperatures between 1700° C and the solidus, the composition of this residual liquid is constrained by the phase diagram (Fig. 1) to be very close to that of the eutectic. In favourable circumstances, this composition can be determined by electronprobe microanalysis. The pockets of interstitial liquid range between 1 and 20 μm and are mostly between 2 and 5 μm in size. Consequently, during electronprobe microanalysis, beam overlap with surrounding metallic iron crystals may often cause the oxygen contents of the pools of quenched Fe–FeO eutectic liquid to be underestimated. Analyses of these regions usually yield a continuous range of oxygen compositions, mostly between 1.0 and 2.2 wt% O. It is believed that the upper limit of 2.2% O (beyond which there is a sharp cut-off) represents the oxygen content of the near-eutectic liquid from which the metallic iron crystals were separating, and that the lower values arise from beam overlap onto metallic iron. At 1700° C, a level of 2.2 w% O corresponds to a metallic liquid containing 10 wt% of dissolved FeO. This is consistent with our previous estimate of the eutectic composition as containing more than 7.5 and less than 12.5 wt% FeO, based upon interpretations of the microstructures of quenched charges. Considered overall, our results indicate that the Fe–FeO eutectic composition at 16 GPa is 10 ± 2 wt% FeO. The metallic iron crystallizing under these conditions typically contains about 100–300 ppm of oxygen in solid solution.

Key runs were also analysed for C, Mg, W and Co which could have been introduced as contamination from the furnace walls and pressure medium. Levels of contamination were below the limits of detection (C < 500 ppm, W < 200 ppm, Co < 150 ppm). These levels are insufficient to cause significant alterations to the phase boundaries shown in Fig. 1.

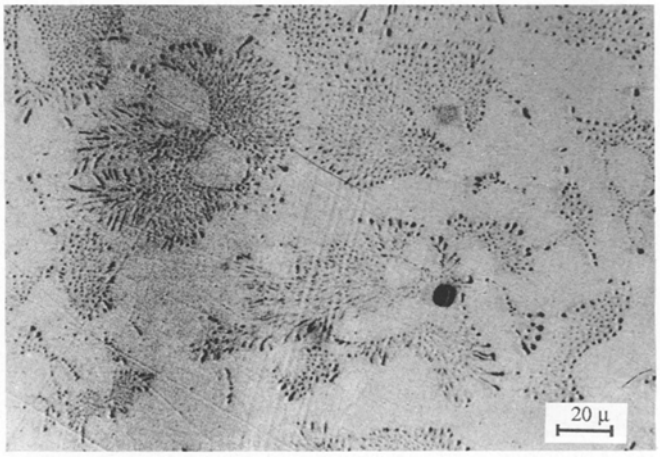

Fig. 7. Backscattered electron image of polished section of run 502 at 1700° C, with bulk composition $Fe_{90}FeO_{10}$. During quenching, oxygen migrates towards boundary of the charge, causing precipitation of crystalline metallic iron (*clear bright regions*). Eventually, growth of metallic iron crystals prevents further diffusion of oxygen and the residual, near-eutectic Fe-O melt then crystallizes within the interstices to form fine intergrowths of metallic iron and feathery FeO precipitates (*dappled regions*). *Large black spots* are holes in the surface of the mount.

Discussion

The temperatures of key phase boundaries in the system Fe–FeO at 16 GPa are found to be substantially smaller than were obtained in the previous reconnaissance investigation by Kato and Ringwood (1989). The present (and previous) results are as follows: (Fe_c–FeO_c) eutectic 1670 (1700)° C, (FeO_c–L_o) eutectic 1760 (1900)° C, Fe_c melting point 1945 (2050)° C. It is clear that the estimation of temperature from power input in the earlier investigation was more uncertain than was believed to be the case. The temperature intervals between runs were also wider in that study. This latter factor is responsible in part for the large discrepancy in the temperatures of the (FeO_c–L_o) eutectic.

The Fe–FeO_c eutectic composition obtained in the present investigation contains 10 ± 2 wt% FeO, as compared to a value within the range 15.5 ± 3 wt% FeO obtained by Kato and Ringwood (1989). We can now recognise that the latter value was too high because of loss of FeO from the charge into the MgO container during the course of the runs. Use of Al_2O_3 containers in the present series of runs has eliminated this source of error.

In the present experiments, we find that 10% FeO has caused the melting point of iron to be lowered by 275° C, which is just within the limits of 350 ± 75° C estimated by Kato and Ringwood. The present experiments yield a lowering of the melting point of iron of 27.5° C per 1 wt% FeO, as compared to 23° C/wt% FeO previously. It is this parameter which is essential for the thermodynamic calculations which were carried out by Kato and Ringwood (1989). The new value agrees with the results of Kato and Ringwood (1989) within

experimental uncertainties, but is believed to be more accurate. The present higher value of the melting point depression implies that the extent the liquid immiscibility field ($L_m + L_o$)of Fig. 1 is significantly smaller than was estimated by Kato and Ringwood (1989). This is also demonstrated by the present estimates of co-existing immiscible liquid ($L_m + L_o$) compositions at 1775° C, as shown in Fig. 1. Apart from these modifications, the key results of the previous investigation are confirmed. These include the large depression of the melting point of iron caused by solution of FeO in the metallic liquid, the large effect of pressure in causing increased solubility of FeO in molten iron accompanied by contraction of the liquid immiscibility field, and the overall topology of the system. The implications of Fe – FeO phase equilibria for the process of core-formation in the Earth as discussed by Ringwood (1984) and Kato and Ringwood (1989) are strengthened by the present results.

The melting temperature of pure iron which we obtained at 16 GPa was 1945° C and can be compared to corresponding determinations (16 GPa) of 1902° C (Boehler 1986)[1] and 1974° C (Williams et al. 1987). However, our measurement does not include the effect of pressure upon thermocouple E.M.F. and until this is evaluated, it would be premature to make a realistic comparison of these results.

On the other hand, our estimate of 1875 ± 25° C for the melting point of wüstite at 16 GPa stands in sharp contrast to the value of 2614° C at the same pressure, obtained by Knittle and Jeanloz (1990) and Jeanloz (1989, 1990). Our result contains an uncertainty owing to the effect of pressure on thermocouple e.m.f. but we doubt whether this would exceed 50–100° C. We have previously observed occasional anomalies (~ 50° C) of melting temperatures in other systems when using MgO capsules, possibly caused by adsorption of water vapour. Although the capsules are thoroughly dried by heating at 1000° C prior to runs and stored in dessicators, they are necessarily exposed to the atmosphere for 1–2 h during assembly of the cells and adsorption of traces of H_2O may occur. However, even the most generous allowances for these sources of uncertainty in our runs do not go far towards resolving the ~ 700° C difference between the present results and those of the Berkeley group on the melting point of FeO at 16 GPa.

Acknowledgements. We are indebted to Mr. N. Ware for the electronprobe analyses and to Dr. S. Kesson for helpful comments upon the manuscript.

References

Boehler R (1986) The phase diagram of iron to 430 kbar, Geophys Res Lett 13:1153–1156

Irifune T, Hibberson W (1985) Improved furnace design for multiple anvil apparatus for pressures up to 18 GPa and temperatures to 2000° C. High Temp High Pressures 17:575–579

Jeanloz R (1989) Physical chemistry at ultrahigh pressures and temperatures. Annu Rev Phys Chem 40:237–259

Jeanloz R (1990) The nature of the Earth's core. Annu Rev Earth Planet Sci 18 (in press)

Kato T, Ringwood AE (1989) Melting relationships in the system Fe – FeO at high pressures: implications for the composition and formation of the Earth's core. Phys Chem Minerals 16:524–538

Kato M, Urakawa S, Kumazawa M (1989) Stability fields of non-stoichiometric wüstite and magnesiowüstite at high pressure. Second Japan-USSR International Symposium on Phase Transformations at High Pressure and Temperatures, Program Abstract 80–81

Knittle E, Jeanloz R (1990) The high pressure phase diagram of $Fe_{0.94}O$, a possible constituent of the Earth's outer core. J Geophys Res (in press)

Ringwood AE (1984) The Earth's core: its composition, formation and bearing upon the origin of the Earth. Proc Soc London A 395:1–46

Williams O, Jeanloz R, Bass J, Svendsen B, Ahrens T (1987) The melting curve of iron to 250 gigapascals: a constraint on the temperature at the Earth's Center, Science 236:181–182

[1] **Note added in proof:** Boehler (pers comm) has recently re-determined the melting curve of pure iron and obtains a melting point at 16 GPa which agrees with the present results